TU DELFT

MSC GEOMATICS THESIS PROPOSAL

ANTRIA CHRISTODOULOU

Image-based method for mobile laser scans registration

Author information:
a.christodoulou-
1@student.tudelft.nl
4620968

Supervisors:
TU Delft:
Prof. dr. ir. P.J.M. van Oosterom,
MSc. R.Y. Peters,
CycloMedia:
MSc. P. Joosten
MSc. B. van Someren

January 14, 2018

1 Introduction

Light Detection And Ranging (LiDAR) sensors deployed on mobile platforms along with Global Navigation Satellite Systems (GNSS) and Inertial Measurement Units (IMU), can be used for the collection of georeferenced (i.e. associated with locations in physical space) 3D point cloud sets of road-side data (Kaartinen et al., 2012). This refers to Mobile Laser Scanning (MLS) systems, with which vast amount of 3D data can be collected in a short time frame by minimum labor force (Mendenhall, 2014). After the acquisition of 3D scans along a vehicle's trajectory, their absolute alignment in a common reference system (global or multiview registration) is required so that 3D representations of the real world's geometry can be constructed. 3D models can be then employed for vehicle and pedestrian navigation, location based services (Kaartinen et al., 2012), disaster management, spatial analysis or even as alternatives to traditional surveying processes. The development of such applications requires automated processing of LiDAR data and therefore automated LiDAR processing techniques are of increasing interest (Kaartinen et al., 2012).

Unification of observations from GNSS and IMU determine the positioning and orientation of the sensor platform (Haala et al., 2008). Specifically, a GNSS provides continuous global positioning using a sufficient number of satellites. An Inertial Navigation System (INS) computes position using accelerometers while the platform moves. In addition, gyroscopes are used to measure the angular orientation of the scanner relative to the ground and also to discard effects of gravity (Levi and Judd, 1996). When Laser scanners support high accuracy acquisition (order of few centimeters), the global accuracy of a MLS system depends on the accuracy of the integrated navigation solution (Puente et al., 2011). However, GNSS visibility may be restricted due to trees and high buildings, thus the number of the employed satellites is not sufficient for positioning calculations. In addition, GNSS signals may be reflected by surrounding structures (multipath) leading to longer traveling times (figure 1) and potentially causing large errors in the position output (Shetty, 2017) . In such cases, the navigation solution of the MLS system depends on the IMU. IMU operate on the basis of the method dead-reckoning (DR), i.e. current vehicle position measurements are based on displacements from an initial known position (Levi and Judd, 1996). As a result, potential error is accumulated and thus the accuracy of the integrated positioning is constantly degrading (Barshan and Durrant-Whyte, 1995).

The construction of 3D models implies sequential registering of all the independently acquired point clouds scans (global or multiview registration). To do so, laser scans with partial overlap, captured at different times, must be firstly registered between them (local or pairwise registration). Partially overlapping views exist when a vehicle returns to a previously mapped region in order to cover a complete scenery of the surroundings. This is quite common in cases of crossed streets. However, due to the potential poor or absent GNSS positioning and due to the IMU operating principle (error accumulation), overlapping scans, which can be more than 2, do not match. There can be translational (X, Y, Z) and rotational (yaw) error between them. The problem of having multiple (partial) overlapping 3D scans acquired at different times as the vehicle had to revisit a previously captured area is known as the loop-closure problem (Bailey and Durrant-Whyte, 2006) (figure 2). This is a local problem since scenes of the same region need to be registered together, but is also directly related with the global registration problem, which requires the alignment of the local sets with the rest of the network.

Matching datasets with overlaps is a major research topic in photogrammetry, computer vision and robotics (Brenner, 2009). Many researches employ a variant of the most commonly used algorithm for local registration of 3D overlapping views, i.e. the Iterative Closest Point

(ICP). These variants deal with the limitations of ICP in order to deliver precise registration of 3D scans. Since these algorithms are based on 3D matching, the computation complexity is high. This research attempts, to solve the registration problem by reducing the dimensions of the problem; by using images generated from the point clouds.

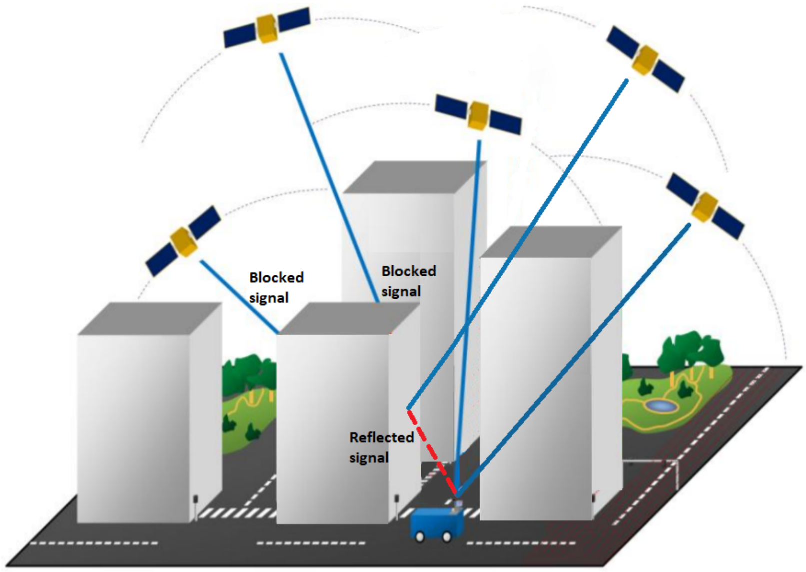

Figure 1: Mobile laser scanning utilizes GNSS-IMU positioning for direct geo-referencing of laser scanning data for 3D mapping. In environments with high-rise buildings or high trees there may be limited visibility of the GNSS signals and/or the signals may be blocked. In such cases the positioning is dependent on the IMU (Modified from (Kukko et al., 2012)).

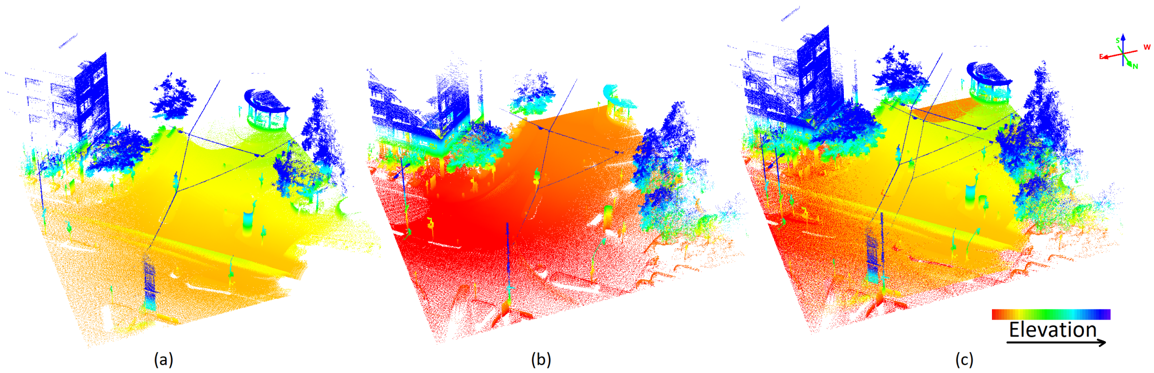

Figure 2: (a) One point cloud tile (50 x 50m), (b) Second point cloud tile from the same region that was captured at a different time and partially overlaps with (a). (c) The 2 point clouds (a) and (b) together, do not match due to the loop closure problem. The differences in the x, y directions are especially visible by looking at the electricity cables. The z difference can be seen by the different color (related to elevation) at the ground of (a) and (b).

2 Related work

2.1 Local Registration with ICP

Local registration methods refer to processes of aligning overlapping scans by estimating the relative transformation needed to match one with another. When the 3D point cloud sets are properly aligned, they are said to be in registration (Magnusson et al., 2007). Many researches employ a variant of the most commonly used algorithm for local registration of 3D overlapping views, i.e. the Iterative Closest Point (ICP). ICP method was firstly developed by (Besl and McKay, 1992) and then several modified versions of this appeared to improve the main ICP algorithm. Researchers usually consider that there is one point cloud set which is 'correct', called target, or model (Besl and McKay, 1992) or reference (Pomerleau et al., 2013) and another one which needs to be register onto the 'correct' one, which is called reading (Pomerleau et al., 2013), or source or data scan (Besl and McKay, 1992). The notation of Besl and McKay (1992) is used here to explain the main ICP algorithm, thus **M** considers the model and **D** the data scan. The ICP algorithm computes the rotation and translation parameters so that **D** aligns best to **M** (Eq. 1), by searching for the correct associations between the points in the two scans.

$$\mathbf{M} = R * \mathbf{D} + t \tag{1}$$

Where R: rotation and t: translation applied to every point in the data scan **D**. To determine the correspondences, each point of **D** should correspond to the point in **M** that results to minimum distance between them (closest point). The purpose is to retrieve a minimum sum of the residuals (Mean square error, MSE) between the corresponding points in the 2 data sets (Eq. 2). In other words, if the correct correspondences are known the MSE should be minimum.

$$\frac{1}{N}\sum_{i=1}^{N}||\mathbf{M}_i - \mathbf{D}_i||^2 \tag{2}$$

Thus, ICP uses the conventional Least Squares (LS) regression method, which is sensitive to outliers. These are observations that do not obey the linear pattern formed by the majority of the point correspondences (Rousseeuw and Hubert, 2011). The algorithms iterates until the MSE is sufficiently small, or the MSE difference between 2 consequent iterations is sufficiently small, or if the maximum allowed amount of iterations is achieved (figure 3). As soon as one of those conditions is satisfied the motion that will match **D** to **M** is calculated (Eq. 3) and applied to **D**.

$$(R, t) = min(\sum_{i=1}^{N}||\mathbf{M}_i - R * \mathbf{D}_i - t||^2) \tag{3}$$

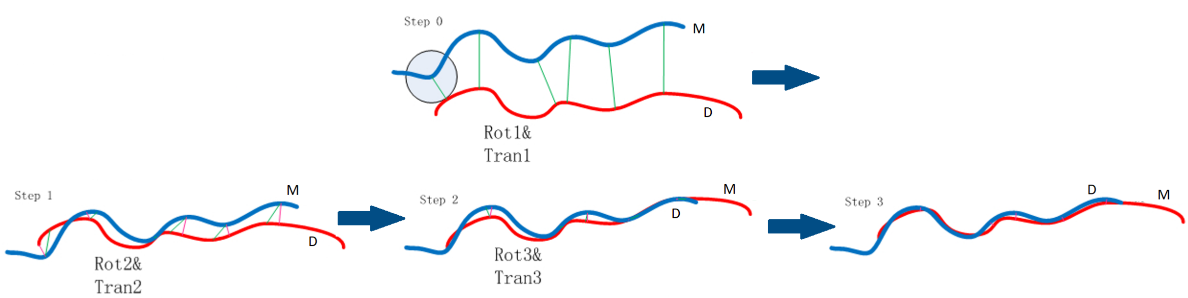

Figure 3: The Iterative Closest Point algorithm that matches the data scan to the model scan by iteratively minimizing the distance between the determined correspondences.

ICP algorithms may vary according to the features registered. For example, the main ICP registers point to point features (Besl and McKay, 1992), Chen and Medioni (1992) register points to planes, Segal et al. (2009) register planes to planes etc. ICP point to point features performs better than the point to plane ICP if there are quadratic or polynomial geometric structures in the scene (Bellekens et al., 2014). ICP point-to-plane (Chen and Medioni, 1992) features can provide better results than the point-to-point if the environment is structured (Pomerleau et al., 2013). Thus, ICP point-to-plane is more suitable for MLS data captured in urban terrains. In cases were a lot of noise is observed in the source point cloud ICP plane-to-plane outperforms ICP point-to-plane (Bellekens et al., 2014).

Variants of ICP provide optimal results when an initial good alignment of the overlapping scans is provided before the actual registration approach is applied (Shetty, 2017), (Cartwright, W. et al., 2009), (Wang C. et al., 2014), (Trucco et al., 1999) (figure 4c). The initial guess in the case of mobile laser scanning is provided by the fusion of LiDAR, INS and GNSS measurements. Namely, the positioning error which leads to the mismatching, provides also the initial information to solve the problem. However, due to the reasons explained, the positioning precision may be limited, thus it is quite common that MLS road-side data provide initial alignment insufficiently precise (figure 4a). ICP methods are also influenced by the amount of outliers with regard to correspondences (Pomerleau et al., 2013). Namely, these are features that do not correspond to the same features in both scans, or features with no correspondence at all due to partial overlap (figure 4b), which is usually the case with MLS data (figure 2). Thus, ICP performs good in cases where all points are in both views (Trucco et al., 1999) (figure 4c). Lastly, as ICP algorithms perform registration in 3D, the execution time of the registration is considerably high (Langerwisch and Wagner, 2010).

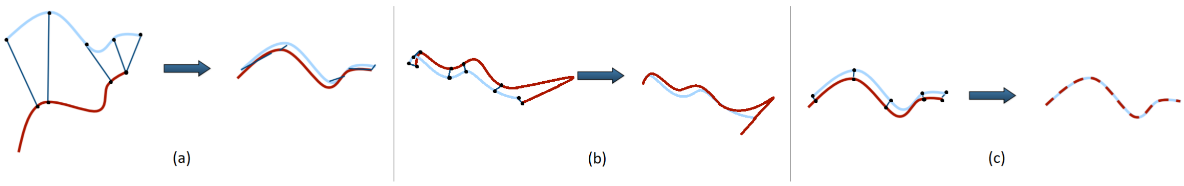

Figure 4: ICP algorithm converges to a false local minimum when: (a) The initial alignment of the two scans is not sufficiently precise, (b) the two scans do not contain the same information (do not fully overlap). (c) ICP algorithm provides sufficiently precise results when the two scans fully overlap and their starting positions are 'close enough'.

2.2 Local Registration with ICP variants

Many algorithms that are based on the main ICP algorithm, attempt to overcome its drawbacks to deliver more robust results. Usually the computation of the correspondences is alternated in order to detect and filter out the inaccurate or/and faulty ones. Some of those algorithms are presented and discussed in this section.

- **Iterative closest compatible point (ICCP) by Guy Godin et al. (1994)**: The difference between the main ICP and the ICCP is that the second searches for the closest point under a constraint. The constraint refers to a compatibility measure with respect to the intensity of the points. If there is a similarity of attributes then the correspondence is accepted else rejected. Among those that confirm the condition, the one with the minimum distance is consider as the closest point. With this technique, the search space of corresponding points is reduced and thus, the most computationally expensive operation of ICP, the detection of correspondences, is improved. In contrast, the sets of closest compatible points are recomputed at each iteration which is quite costly operation. ICCP also suffers in the same manner as ICP from the effects of partial overlap between the compared scans.

- **Robust ICP (RICP) by Trucco et al. (1999):** The difference of RICP and main ICP is that LMedS (Least Median Squares) method (Rousseeuw, 1984) is applied to eliminate the outlier correspondences. A point from each point cloud set is randomly selected, their registration transformation is executed ($\mathbf{M} = R * \mathbf{D} + t$) and then their residual is calculated. This process is repeated until all the potential registrations are evaluated and the one that returns the minimum median residual value is chosen. The residuals that are larger than a given by the user threshold are rejected. RICP also depends on the approximate initial alignment as the main ICP. Nevertheless, it provides good results (better than main ICP) if there is a high presence of outlier correspondences (i.e. large partial overlap).

- **Trimmed ICP by Chetverikov et al. (2002):** The trimmed-ICP algorithm is based on the Least Trimmed Squares (LTS) method which was introduced by (Rousseeuw, 1984). This method takes into account the distances between corresponding points in point cloud pairs. It sorts the square distances and minimizes their sum by iteratively excluding a certain amount of extreme values (Chetverikov et al., 2002). Thus it trims the smallest and largest residuals of distances to prevent influencing the point cloud registration. It is proven by Rousseeuw and Leroy (2005) that LTS can reach its optimal properties with a trimming constant h $(n/2 \leq h \leq n)$ equal to $(n/2) + (p + 1/2)$ (Víšek, 2012), where p refers to the number of explanatory variables. The optimal properties of LTS relate to its highest breakdown point which is equal to 50%. Breakdown point is the degree of robustness of an estimate in the presence of outliers. It measures the amount of outliers an estimate can handle before giving a spoiled estimate (Hampel, 1971). The advantage of this method is the high breakdown point of LTS, which means that Trimmed ICP can handle highly contaminated data (Čížek and Visek, 2000). In contrast, a limitation of this method is that it assumes a fixed overlap of scans (Pomerleau et al., 2013), i.e. Knowledge about the overlap is necessary or has to be estimated to know how many point correspondences to trim. Also, the overlap between the pairs should be under 50% Chetverikov et al. (2002), while less than 40% is not recommended (Padia and Pears, 2017). These are hard to control with a mobile platform. In addition the sorting of the point correspondences by distance and removing a portion of them, adds to the computational load (Padia and Pears, 2017).

- **ICP Registration Using Invariant Features (ICPIF) by Sharp et al. (2002):** This approach deals with the improvement of correspondences selection by extracting features from the point clouds using shape descriptors. Then they use point positions related to the features to extract the correspondences. The features that they extract are invariant to 3D rigid motion (do not change when arbitrary rotations and translations are applied). Such features are the curvature (amount by which a geometric object deviates from being a flat plane, or a curve from being a line) and second order moment invariants in 3D (specific quantitative measure of the shape of a set of points). After the invariant features extraction in both point cloud sets, an iterative algorithm is set which computes the correspondences between the invariant features like the main ICP. The benefit of this algorithm is that fewer iterations of the algorithm are needed to achieve the 'ideal' registration than the main ICP algorithm. However, the ICPIF construct correct correspondences under noise-free conditions and most important it is stated that the results are sufficient for coarse registration than fine registration.

2.3 Image based registration of 3D point clouds

Point cloud registration methods using images is not a common approach. However, in a method of (Lin et al., 2017), firstly bearing angle images (see Section 4.2) are generated from the 3D point clouds to highlight the edges formed by angles in diagonal directions and then a feature based matching method is used to find corresponding pixels between an image pair. Thereafter, only 50% of the best corresponding pixel pairs are used, then the method traces back to the 3D coordinates of the correspondences and lastly those are used in a least squares approximation to derive the transformation parameters. The benefits of this method are that initial alignment is not needed and the computation cost is significantly less than ICP, due to the 2D matching. However, the precision is not better than that of generalized-ICP (plane to plane).

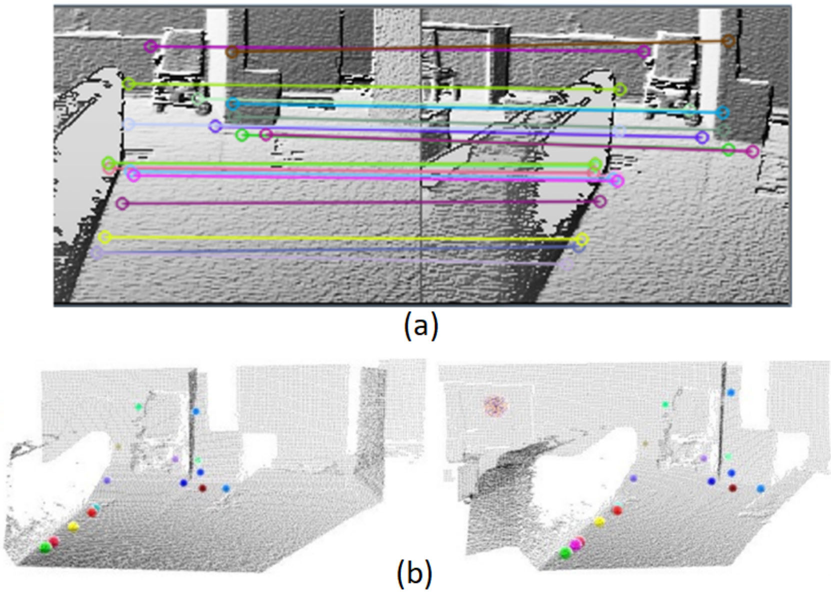

Figure 5: (a) Two bearing angle images that highlight the edges of the objects in the diagonal direction, extracted from a two point clouds. In addition, the correspondences found in the images by using a feature descriptor are shown. (b) The correspondences found in 2D, traced back and presented in the 3D space (source (Lin et al., 2017).

Furthermore, in a method of Langerwisch and Wagner (2010), 2D virtual scans are extracted from indoor point cloud scenes, registered using ICP and lastly, the transformation parameters used to align the images are converted to 3D. The basic idea of their algorithm is that the 6 degrees of freedom (DoF) transformation in 3D (they consider apart from translation in the 3 directions, yaw, pitch and roll) can be split in several transformations of lower dimensions. The single transformations are combined subsequently to gain the full 6 DoF transformation. The innovative characteristic of this method is that the 3 rotational angles of the 3D space can be detected using 2D images. Precisely, three 2D images are extracted, one along the x-y plane, one along the x-z plane and one along the y-z plane for each 3D scan (Wulf, 2008)[1]. Due to that yaw, roll and pitch can be determined in 2D, along with X, Y, Z translation. Another advantage of this method is that the computational load is decreased since correspondences are searched in a 2D space. However, 3 images need to be generated from each point cloud scan, and as it constitutes an ICP method, an initial alignment is necessary to retrieve precise results.

[1]Wulf, O. (2008). Virtuelle 2D-Scans - Ein Verfahren zur echtzeitfahigen Roboternavigation mit dreidimensionalen Umgebungsdaten. PhD thesis, Leibniz Universitat Hannover, Hannover, Germany. This reference is in German and therefore no more information about the technique used to generate the 2D virtual scans could extracted.

A method developed by (Liang et al., 2017) retrieves perspective intensity images by applying central projection of the terrestrial LiDAR data from a viewpoint (see Section 4.2 and employs corner points in the images as tie points to acquire transformation parameters. Thus, intensity is used to reflect the appearance and the geometric structures of objects in order to extract feature points and apply point cloud matching. The advantage of the images used for registration over a 3D solution is that details of building structures are usually more distinguishable (Liang et al., 2017). In contrast, one should generate perspective images from many viewpoints to achieve complete representation of the 3D point cloud sets.

3 Research Objectives

3.1 Objectives

The goal of this research will be to study and assess the potential of solving the pairwise registration problem of Mobile Laser Scans scans using images. By converting the 3D data to imagery there is however a direct disadvantage; the loss of information. Firstly, because by converting to 2D imagery the view of the data is limited in 2 directions. Secondly, the resolution of the generated images may be a reason for the information compression. Nevertheless, it is believed that the loss of information can be partially beneficial. Namely, the loss of information may be useful for hiding outliers. These can be points that were captured at one of the 2 scans due to the different scanning views and points of objects that do not belong to the topography of the environment but were present when one of the 2 scans was retrieved. Moreover, by using images the computational efficiency could be decreased, which is important since road-side data acquisition means vast collections of 3D point clouds. In addition, it has been proved by many ICP variants that registration of 3D data in 3D requires a good initial estimation of the overlapping scans position, else the algorithm minimizes the MSE but by associating wrong points. In other words, the search space for correspondences should be relatively small. Contrarily, there are image registration methods such as template matching (meant for matching patch images to bigger images - see Section 4.3) with which is believed that the tolerance to the size of the search space could possibly be high.

Therefore the main research question for this thesis is formulated as follows:

To which extent is it possible to automatically, efficiently, precisely and robustly align mobile laser scanning data relatively, using an image-based technique?

To achieve this, the following sub-questions are relevant:

- How to deal with the outliers in the data so that they do not affect the registration?
- How to generate images and what kind of images so that the 3D point clouds are best described?
- How to locally solve translation and rotation (yaw)?
- How to assess efficiency, precision and reliability of the developed method automatically?

3.2 Scope of research

This thesis will focus on how to match overlapping scans using images as an intermediate step and how to evaluate automatically the robustness, precision and efficiency of the method. It is of high importance to gain insight on the quality of the to be developed method by means of statistics. Furthermore, this project will not deal with the global alignment problem to align all the scans from a region in one common reference system.

4 Methodology

For every step of the methodology note that the data that will be used comes in forms of tiles of 50 by 50 meters. The methodology steps are presented on figure 6 and explained in this section.

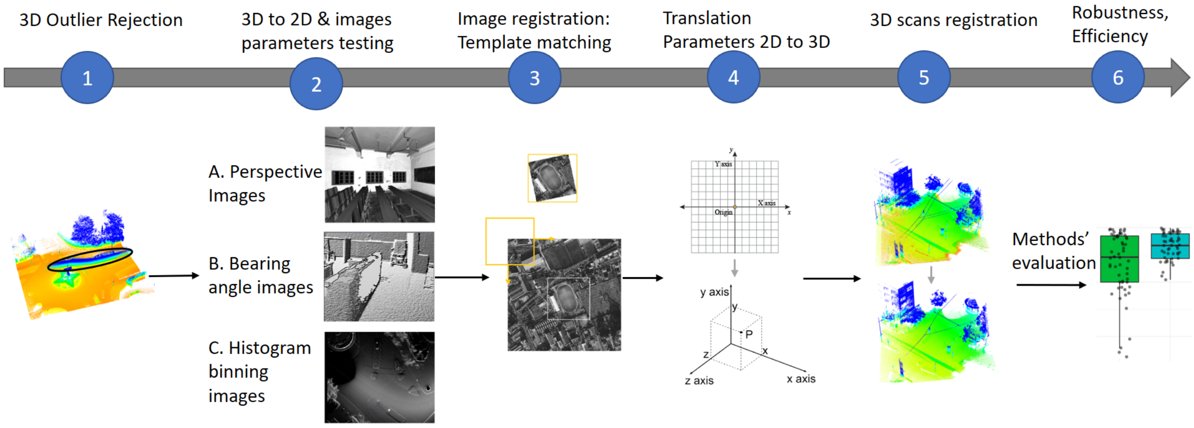

Figure 6: A flowchart presenting the methodology steps of this thesis project.

4.1 Preprocessing: Outliers Rejection

The first step of this project will be to reject the outlier points in each point cloud scan so that they do not affect the registration performance. The appearance of outliers can cause convergence of a registration algorithm to an optimum solution, which is driven by false matches. Therefore, outlier removal is considered essential for a point cloud registration process. Firstly, it is necessary to explain what an outlier value represents in LiDAR data, regarding the problem of matching LiDAR scans captured at different times:

- Outliers can be points that do not appear to both scans, because the 3D scans were retrieved from different angles. These are not real outliers of the data (but partial overlap). In Section 2.2 is discussed that ICP variants deal with outlying correspondences, as ICP algorithms perform optimally if all points are in both scans (Trucco et al., 1999). Namely, this is partially related to the definition of outliers provided here (figure 7a).

- Outliers can be points that do not appear to both overlapping scans although the scans cover the same area, because these points do not belong to the topography of the interested area (Matkan et al., 2014). These can be clusters of points or single points (Pang, 2011). Examples of clusters could be cars, people, high elevation values that are resulted from birds or other suspended objects at high altitude, such as smoke (Matkan et al., 2014) (figure 7b). Also, when the laser beam hits the boundary of a 3D-object, but that object blocks others (with respect to the laser beam direction), then points appear in between the 2 objects. The reflected flux of these points is a weighted average of the reflected flux from the 2 objects (Sotoodeh, 2006). Single outliers appear in cases of surfaces that return very high or very low reflectance values (e.g. black objects, glasses and slick

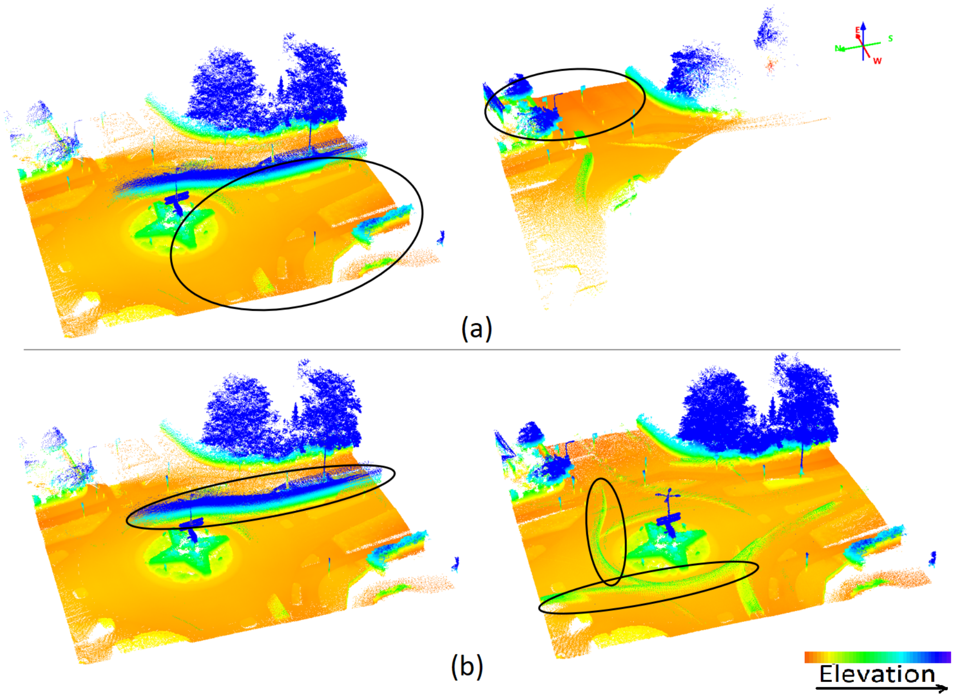

Figure 7: (a) Points in black circles indicate areas which do not appear in both overlapping scans due to capturing from different angles. These points consider as 'outliers' in registration processes. (b) Points in black circles are outliers in general in LiDAR data, as they do not belong to the topography of the area. Here we see cars in motion.

metal surfaces) (Sotoodeh, 2006). This results to biases in distance measurements and thus to increased noise (Beraldin, 2004). In addition, in cases were objects are hit under a low angle, the laser beam is firstly deflected onto neighbor objects and then reflected back to the receiver causing longer travel time of the laser beam (Sotoodeh, 2006).

In this project, a method will be applied to reject the actual outliers in the LiDAR data, those that are not part of the natural and artificial physical features of an area (second category, figure 7b). Only this category is considered because it can highly affect the matching since it refers to wrong information. The first category, the partial overlap, refers to additional information in one of the scans, which may confuse the image matching if the environment is very cluttered, but not necessarily cause incorrect registration. Furthermore, it is not the focus of this project to detect the ideal method to reject the outliers, however it is part of the problem and thus a technique will be applied to attempt to solve this.

Matkan et al. (2014) deal with single and cluster outliers. They use a cross-validation technique and specifically the method leave-one-out method. Every data point of a LiDAR point cloud set is selected once as the testing sample and excluded from the rest of the dataset. Then Inverse Distance Weighted (IDW) interpolation is applied to the height of the surrounding points of the selecting point to find its interpolated height. The error of this point is calculated by subtracting its actual height from the predicted height. After applying this process to all the points, a threshold is determined based on the maximum error value, and the points that gave an error value higher than the threshold are rejected. The cross validation process is repeated and the algorithm terminates when the maximum height error value is higher than the maximum error of the previous iteration. This method does not require ancillary data, and the chosen cross validation method is less biased than others as every sample is considered as a test. However, it is very computationally expensive since every point is taken as a testing sample. Also, this method reject outliers based on the neighboring values of a point and as a result, if there is a big cluster of outliers then the sample point will be considered as inlier. Thus this method will not be used or further researched.

(Pang, 2011) uses a Minimum Covariance Determinant (MCD) which is applied onto a multi-attribute model. The elevation of each point is used as the location attribute. A Connectivity Outlier Factor (COF) that indicates how isolated a point is from its neighbors, is used to describe a spatial neighborhood relation attribute. These 2 attributes of each point are combined to form a 2D space (figure 8a). The COF together with the height of each point are used in the MCD-based model. MCD is a robust estimator of location and scatter (Rousseeuw, 1985), in comparison with sample mean and the sample covariance matrix, which are highly affected by outliers (Pang, 2011). The MCD of a dataset refers to the minimum number of points that are not outliers. The MCD is applied by using a robust Mahalanobis distance measure, that considers the average value, the variance and covariance of the attributes measured. Outliers are considered the points of which the Mahalanobis distance value is larger than a given threshold (figure 8b). This method can detect most of the individual and cluster outliers. However, points with not very low or very high elevation (that probably have high COF) are considered as outliers. Similarly, points with not very high COF (that probably have high elevation) are considered also as outliers. Nonetheless, considering more points as outliers than they actually are, could increase the efficiency of the registration process. However, this should be balance, as considering high amount of points as outliers may lead to less precise results.

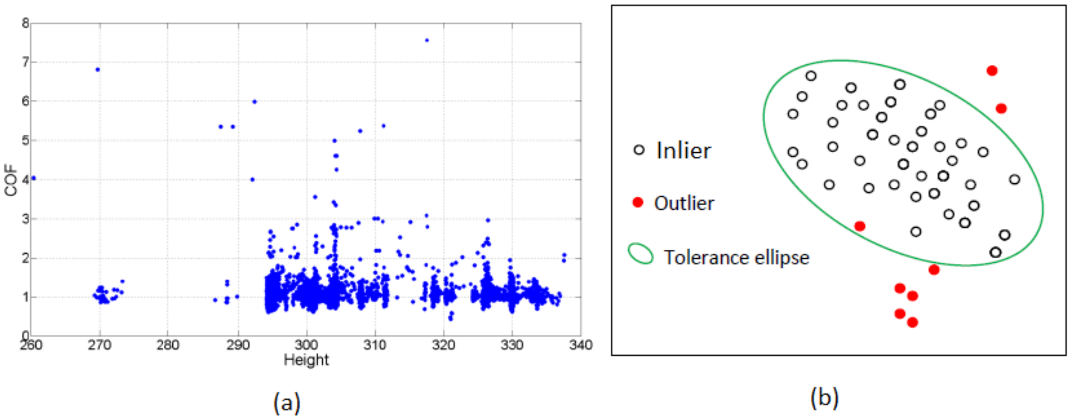

Figure 8: (a) Formed 2D space based on the elevation and COF. (b) A Robust Mahalanobis distance is applied on the 2D space and calculated for each point to measure how far a point is from the mean, the variance and covariance of the distribution of the calculated attributes. If the Robust Mahalanobis distance is higher than a threshold then the point considers an outlier.

The method that will be used in this project for outliers rejections will adopt ideas from the method of Pang (2011). A multi-attribute model will be developed and it will be formulated by a factor to determine how isolated a neighborhood is form other neighborhoods and a density factor to determine the relative density deviation of a local neighborhood. By including the density will allow to observe neighborhoods' consistency. By assessing the data in spatial groups, instead of doing it individually, the X and Y information is not neglected. In addition, the formulation of neighborhoods and the calculation of attributes for the neighborhoods leads to the creation of clusters. Therefore, criteria for points removal will be assessed based on the clusters and not based on the distribution of the rest of the points in the multi-attribute space. Instead of using a Mahalanobis distance, other criteria that are insensitive to high dimensional space will be employed to detect if whole clusters or some points from clusters should be removed.

4.2 From 3D point clouds to imagery

After outlier rejection, the next step will be to convert the 3D point clouds to images. Different images techniques that are discussed and compared in this section, will be also implemented and evaluated.

An option would be to construct depth images. To do so, the distance between the viewpoint and the point on the object surfaces is needed (figure 9). Computational efficiency is the advantage of this kind of images, since the transformation from 3D to depth images is simple and fast. However, depth images discard important geometric information, as it is for example the relation between neighboring points, which could limit the registration performance (Lin et al., 2017). Thus they won't be used in this project.

Figure 9: The figure represents a depth image. Objects that are further away from the viewpoint appear with darker color, while objects closer to the viewpoint appear brighter.

Another option would be to use spin-images, which can also be used as features descriptors (see Section 4.3). Spin images, introduced by (Johnson and Hebert, 1998) and encode the properties of surfaces in an object-oriented coordinate system. By using these systems, the description of a surface does not change as the viewpoint changes. To generate a spin image, a 3D surface point with its associated direction (normal) is used. The surface to which this point corresponds is represented as a polygonal mesh with vertices. Then a tangent plane through the observed point and perpendicular to its normal is used, along with a line parallel to the normal. As a result, a (α,β) cylindrical coordinate system is created, where α is perpendicular distance to the normal and β the perpendicular distance to the constructed plane. Then a spin image can be expressed as the projection of 3D points to the 2D coordinates (α,β) (figure10a). To actually create the spin image a grid is constructed and the amount of 2D points falling into each grid cell is used as the image value (Johnson and Hebert, 1998) (figure10b).
Spin images can be used for surface matching (Johnson and Hebert, 1999). Spin images from points on one surface are constructed, and then a vertex from the other surface is randomly selected, its spin image is constructed and compared using a correlation coefficient with the images of the other surface. To retrieve a full representation of a surface, spin images must be created for all the oriented points that are defined by the surface mesh (Johnson and Hebert,

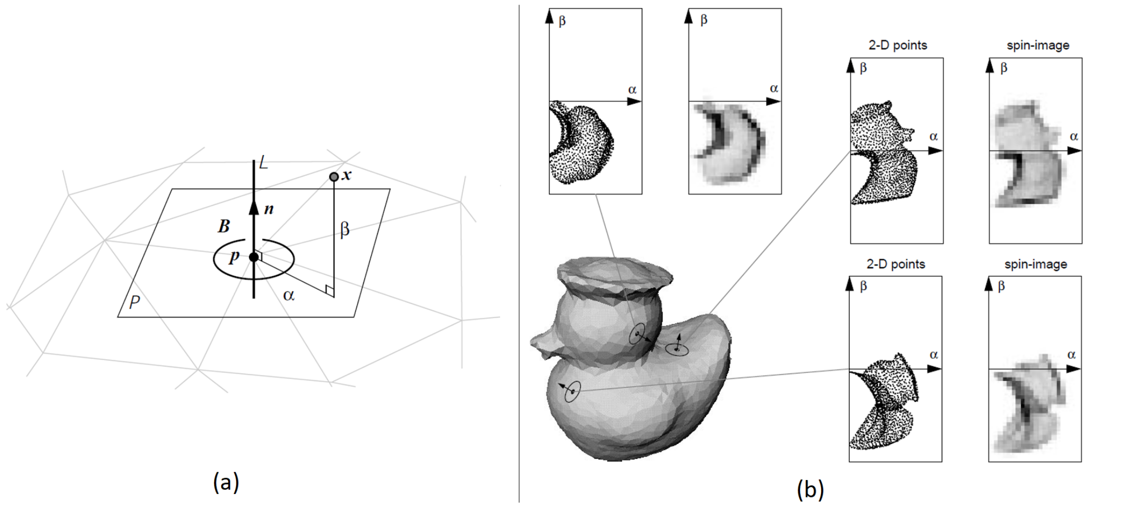

Figure 10: (a) The figure shows the α,β cylindrical coordinate system created at a vertex in a surface mesh (where α the radial distance to the surface normal line and β the axial distance above the tangent plane P). The position of the oriented point is the 3D position of the vertex and its direction is the surface normal at the vertex. (b) The 3 spin-images generated from 3 oriented points on the surface of a model (source (Krause, 1997).

1999). The disadvantage of this method is that this process needs to be iterated for many points, which would make the computational load very heavy. Spin images will be assessed for registration performance, only if there is a way to combine the images from several oriented points of a 3D scan into one entity.

Another method that will be used to convert 3D to 2D is the perspective intensity images (used by Liang et al. (2017)). Their generation requires the use of the collinearity equation (which is commonly used in Photogrammetry) to calculate the corresponding planar coordinates from the 3D points clouds. Namely, the resulted image is a central projection of the 3D space observed from a center of projection (figure 11). This, could be the laser scanner pose location (trajectory point) related to each scan. Another idea which could be evaluated would be to extract perspective intensity images by using synthetic projective centers, in line with the idea of Langerwisch and Wagner (2010) presented in Section 2.3. Namely, to acquire a set of 3 images, one for the x-y plane, one for the x-z plane and one for the y-z plane. The question then is, from which side of the point cloud to place the projective center in order to extract the x-z and y-z image? If an inconsistent way of doing this is applied, then there will be no common information between the overlapping scans and the registration will not be feasible. Nevertheless, having 3 scans instead of one per point cloud could provide more information regarding the spatial relationships of the objects in the images. Also, with this way we could get same translation parameters twice, e.g. x translation from xy and xz. This will allow for the results verification. Lastly, a gray value will be calculated for the projected points based on their intensity with respect to the 3D point cloud. It is important to mention that it will be a bit complicated to trace back to 3D the translation parameters in pixel coordinates due to the complexity of the collinearity equation and the (to be chosen) perspective center.
The third method to construct images will be the bearing angle images which were proposed by (Scaramuzza et al., 2007). These represent the gray level images composed by the angle between the laser beam and the vector that joins 2 consecutive points. One can choose the directions of the 2 consecutive points by deciding along which direction is desired to highlight the details of the scene. The computation of the bearing angle value is a function of the depth

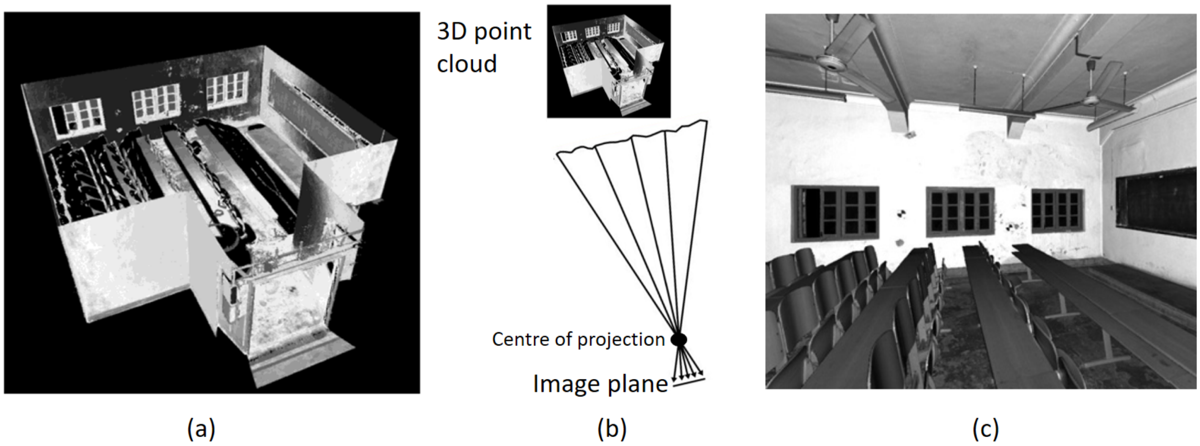

Figure 11: (a) A screen-shot of a point cloud. (b) Central projection applies on the point cloud from a center of projection, which is placed inside the scene of the point cloud in (a) and lies on the same direction as the one shown in the image (b). (c) The retrieved image.

value of a point, the depth value of its adjacent measurement point, the distance between the two and the angle in the selected direction (e.g. vertical, horizontal, and diagonal) (figure 12). Thus, the benefit of a bearing angle image is the capability to highlight depth discontinuities and direction changes of the scene. By adopting this, the assumption that consecutive points hit the same surface is made. But if this is not the case, details in the images, such as edges, are inaccurately highlighted. An idea to improve the principle behind the bearing angle image construction, would be to involve the normals of the planes. Specifically to compute the bearing angle value between the normal and the laser beam.

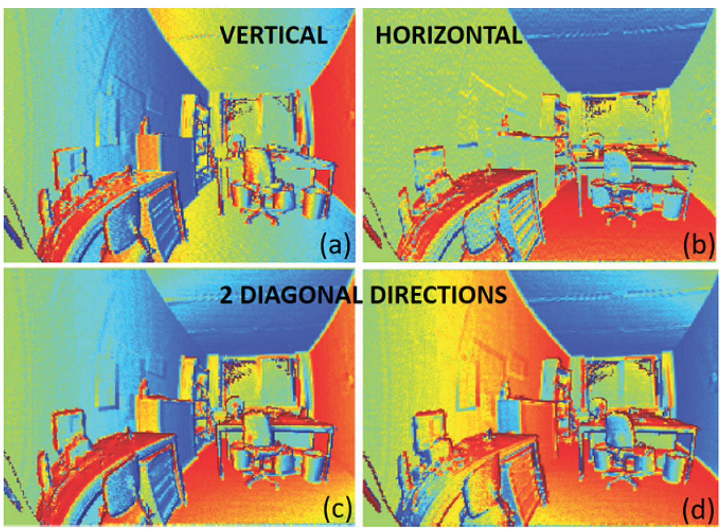

Figure 12: (a) Bearing angle images in the vertical direction, (b) the horizontal direction (180 deg), (c) and (d) in the diagonal directions (-45 deg, +45 deg). The color shade added from blue to red,is proportional to the bearing angle value (source (Scaramuzza et al., 2007)).

The last method that will be used and assessed for its performance, is the histogram binning method. Similar ideas to this approach are described by (Blomley et al., 2014). Specifically, a set of 3 images per point cloud will be created, one for the x-y plane, one for the x-z plane and one for the y-z plane. Each one of those planes is gridded and the corresponding point coordinates to the constructed plane (e.g. x and y for plane x-y) are binned into the cells . Specifically, the value of each pixel represents the frequency of points fall within the corresponding 2D grid cell. For example, for the creation of the x-z image, a point cloud is projected to the vertical plane x-z, that plane is divided using a grid. Each grid cell corresponds to a bin in the x-z histogram and/or a pixel in the x-z histogram image. The same idea follows for the other 2 images (figure 13). With the binning histograms method, information is decreased as points are binned in cells and thus the exact location is missed. Nonetheless, relationships between objects are still visible and more important these images indicate clearly when a field is empty or when there is a wall, which can be useful during the matching of the 3D scans.

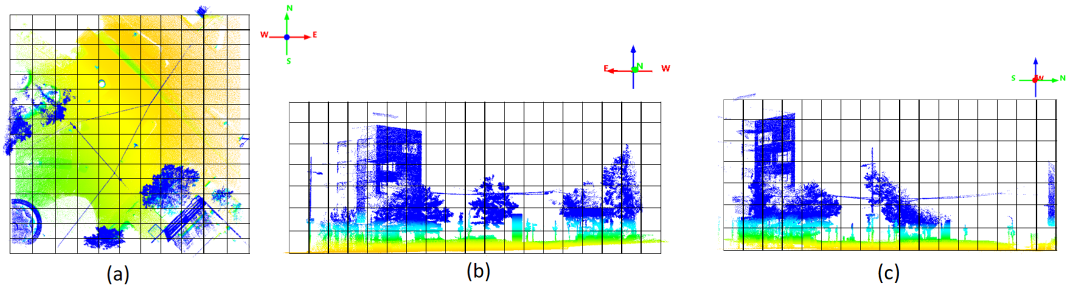

Figure 13: (a) The x-y plane of a point cloud tile, gridded to accumulate the number of points in each cell based on x and y. (b) The x-z plane of a point cloud tile, gridded to accumulate the number of points in each cell based on x and z. (c) The y-z plane of a point cloud tile, gridded to accumulate the number of points in each cell based on y and z.

The advantages and disadvantages of the image techniques discussed are summarized in Table 1. It is noted that, for all the kind of images that will be used, different pixel size values will be assessed to test how the performance of the registration modifies.

4.3 Local Registration

The next step will be to register the images in pairs. The registration will be performed by using the images retrieved for each of the 3 techniques mentioned in Section 4.2, for the 3D conversion to 2D. At the end, the results provided from the different solutions will be compared. There are two methods that could be used for the image registration in order to acquire the alignment transformation parameters.

1. **Feature Extraction:** The first method is the extraction of features from the images and the use of those to determine the matching. This requires the employment of feature detectors in order to locate distinctive elements in the image. These can be for example blobs in the images, corners, lines, junctions in 'T' shape. It is important that a feature detector can find the distinctive elements in the images under any viewing conditions. Feature detectors can thereafter be used by feature descriptors to represent the pixel region surrounding the 'interest points' using vectors. Lastly, the descriptor vectors can be utilized as discrete correspondences between two images, so that matching can be applied based on a distance between the them (Bay et al., 2008).

2. **Template Matching:** The second method that could be used for pairwise registration is the template matching. This technique compares a template image (usually sub-image/patch image) over a reference image to identify the location of the template into the reference (Wei et al., 2014). A window with the same size as the template is slided over the reference image. Then similarity values are computed between the template and the reference to detect the window that is most similar to the template. In other words,

Table 1: Comparison of the image techniques for the conversion from 3D point clouds.

3D to 2D Image Techniques Comparison	**Images**				
	Depth	**Spin**	**Perspective**	**Bearing Angle**	**Histogram Binning**
Advantages	transformation 2D to 3D simple & fast	shape descriptor	if 3 images: x-y, x-z, y-z from each scan, then translation parameters twice	highlight depth disconti-nuities (correctly) if assumption is valid	objects' relationships visible
			information about objects' spatial relationships	highlight orientations of structures (correctly) if assumption is valid	give strong signals when there are walls or empty spaces
Disadvantages	discard of geometric information	time costly registration: 1 image per oriented point	critical selection of projective center	direction/s to stress the details should be chosen	exact location is missed
	objects' relationships difficult to be seen	many images per 3D scan: complexity	complexity of tracing back to 3D	if consecutive points not on same surface then details inaccurately highlighted	

the matching location based on the highest similarity (or lowest distortion, depending on the method) determines the point where the shape given by the template lays inside the reference image (Swaroop and Sharma, 2016) (figure 14). Template matching techniques are used also for matching images of the same size (Ding et al., 2001). What changes is that a border should be added in one of the two images so that there is enough search space to slide and detect the template. The other idea is to create sub-image of the one image and use that as a template. There are methods that are used to define the location of the template if only translation needs to be solved, but simultaneously can tolerate small rotational angles between the template and the reference image. Tolerance can be increased if some blurring is applied onto the images (Ding et al., 2001). Thus, a method to define the approximate location of the one image into the other could be applied after some blurring of the images. As a result the approximate matching location is obtained (translational parameters) and thereafter a method to detect the rotation could be utilized. For detecting translation, the commonly used method cross correlation could be applied (Swaroop and Sharma, 2016) and for the rotation a method using orientation codes (Ullah and Kaneko, 2004) or a polar transform (Matungka et al., 2009).

There are many algorithms developed for feature extraction, in 3D and 2D. Some of those algorithms are specialized on detecting trees, others on poles, buildings etc. For the purpose of matching laser scanning data, a feature extraction method should have the ability to marked out the important pieces of information in every terrain (either there are only trees or only urban structures). In comparison, a template matching technique does not rely on additional processes, as it only compares the 2 images between them and tries to detect where the maximum similarity is placed. Therefore, the template matching technique will be used in this project for the pairwise registration process.

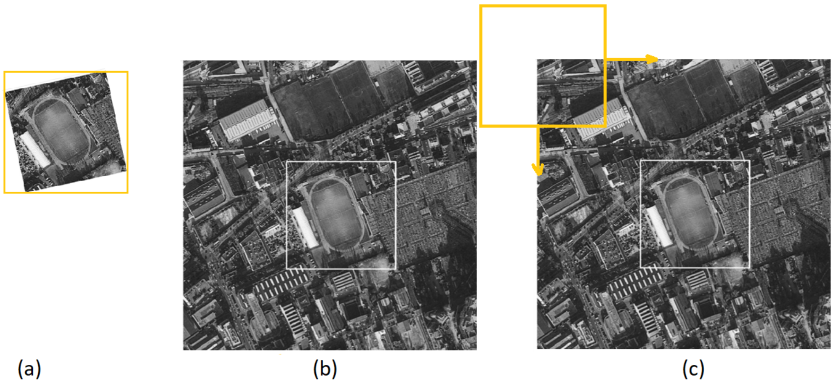

Figure 14: (a) A template image. (b) A reference image in which the location of the template is indicated. (c) A window of the template's size is slided over the reference image to detect where the highest similarity between the template and the reference image lays.

By applying template matching, the 2D transformation parameters that match the images are obtained. The next step to apply in order to perform 3D pairwise registration between scans captured at different times, will be to convert the translation (X,Y,Z) parameters from the 2D pixel coordinates to the 3D reference system coordinates. This is dependent on the image method technique. For example, for the perspective images the collinearity equation will be used to trace back to 3D, as it will be used to retrieve the 2D coordinates. For the histogram binning method, the matching location will have to be multiplied by the bin width. If a border is added on the reference image, then this is modified.

It is marked that after the pairwise registration, a global registration process should follow, which is however outside the scope. A global registration method deals with all the scans retrieved from an area and attempts to solve the loop closure problem (overlapping scans captures at different times). A way to solve this is by using the Pose Graph Optimization method. Namely, all the possible pairwise registrations should be first detected by using some constraints. For example, one scan may be registered with another if it is placed not further than a certain distance, if the acquisition time difference is not higher than a certain time etc. Then a list with possible registration pairs is obtained. Thereafter, this list is filtered based on some indicators to reject the registration pairs that are very unlikely to be correct, they have for example very small overlap. Then the local registrations would be performed based on the template matching method. Subsequently, the individual solutions retrieved would be used as positioning constraints within a pose graph. Constraints would represent also the IMU positions and GNSS positions of the scans. Then weights are attached to each of the input of the three cases. A pose graph attempts to pulls the positions of the scans based on the 3 positioning constraints so that an optimal graph with the scans' positions is obtained.

4.4 Method's robustness evaluation

The last step of this method will be to assess the robustness, precision and efficiency of the solutions developed with different image techniques.

The robustness of an algorithm in the case of overlapping scans registration relates to:

- the verification of the algorithm's performance in several conditions He and Mei (2015). For example, by using different data (urban, forest terrain), particular structures (tunnels), diversity of terrains smoothness (flat surfaces vs surfaces with slope), different LiDAR sensors.
- the verification of the algorithm's insensitivity to doubtful elements He and Mei (2015). For example noise, outliers.

Therefore, some of those cases will be tested so as conclusions can be extracted about the strength of the to be developed methods. Namely, the pairwise registration methods' will be tested:

- in different distances covered by the vehicle. The translation error that will be extracted from each matching is not related only to the relative positioning, but also to the absolute positioning since the error propagates. This relates to the distance covered by the vehicle.
- in different countries. This is necessary as in each country, same kind of terrains, for example urban areas, could be rather different.
- for many cases of different kinds of environments (urban areas, areas with many (high) trees) and for many cases of structural particularities (e.g. tunnels, bridges that 'intersect', urban areas with water nearby (e.g. from a canal)).

To do so, a land use layer (to obtain information about the terrain), a road network layer (to detect streets intersections as these are the most common cases where scans from different times can be found) and another layer with large scale data (to get information about structural particularities) will be used. These layers will be intersected with the laser scan positions so that a big amount of scans for each of the cases are gathered. For instance, an intersection will be applied between the crossed streets, the urban areas that have high buildings and the laser scan positions. That will allow to perform registration with the 3 methods (see Section 4.2) to a large amount of scans that capture areas with high buildings. As a result, it will be possible to report the time needed and extract statistics about the precision and the consistency of the positioning errors detected with each of the developed methods. Apart from this, statistics will be reported with respect to the distance covered, thus registration will be applied to the scans captured after short distance covered and long distance covered by the vehicle. With the described technique a clear idea about the robustness of the methods' will be acquired.

5 Time Planning

The time schedule in figure 16 and the list in figure 15 indicate a planning of the required activities in order to achieve the goals of this project. These, may be alternated based on the research and the initial results.

Image based registration of 3D MLS scans

P1	**100%**		**Start**	**Due**
Select thesis topic	100%		9/26/17	11/13/17
P2	**81%**		**Start**	**Due**
Study Mobile Laser Scanning	100%		11/14/17	11/19/17
Study other pairwise matching algorithms	100%		11/20/17	12/1/17
Study outliers detection	80%		12/4/17	12/8/17
Study 3D to 2D techniques	100%		12/11/17	12/22/17
Study image registration methods	80%		12/26/17	12/31/17
Study Global registration and loop closure	50%		1/1/18	1/7/18
Study robustness	50%		1/8/18	1/11/18
Writing Report	90%		1/1/18	1/12/18
Presentation & Preliminary data	0%		Yesterday	Wednesday
P3	**0%**		**Start**	**Due**
Extra research outliers	0%		Thursday	Saturday
Extra research robustness & rotation template	0%		1/29/18	2/2/18
Reject outliers	0%		2/5/18	2/16/18
Develop bearing angle images	0%		2/19/18	3/2/18
Parameters Testing & Registration	0%		3/5/18	3/9/18
Develop perspective images	0%		3/12/18	3/23/18
Parameters Testing & Registration	0%		3/25/18	3/28/18
Parallel Writing	0%		2/5/18	3/28/18
P4	**0%**		**Start**	**Due**
Develop histogram binning images	0%		3/29/18	4/3/18
Parameters Testing & Registration	0%		4/4/18	4/13/18
Robustness	0%		4/30/18	5/18/18
Presentation preparation	0%		5/18/18	5/25/18
Parallel writing thesis	0%		3/29/18	5/29/18
P5	**0%**		**Start**	**Due**
Thesis corrections after P4	0%		5/29/18	6/15/18
Thesis Final document	0%		6/16/18	6/29/18

Figure 15: Time planning of the required activities and their starting and ending dates.

This thesis is in cooperation with the company CycloMedia. It is noted that weekly meetings will be held with the supervisors from the company and every two weeks with the two supervisors from TU Delft, preferably together so that feedback is provided from both.

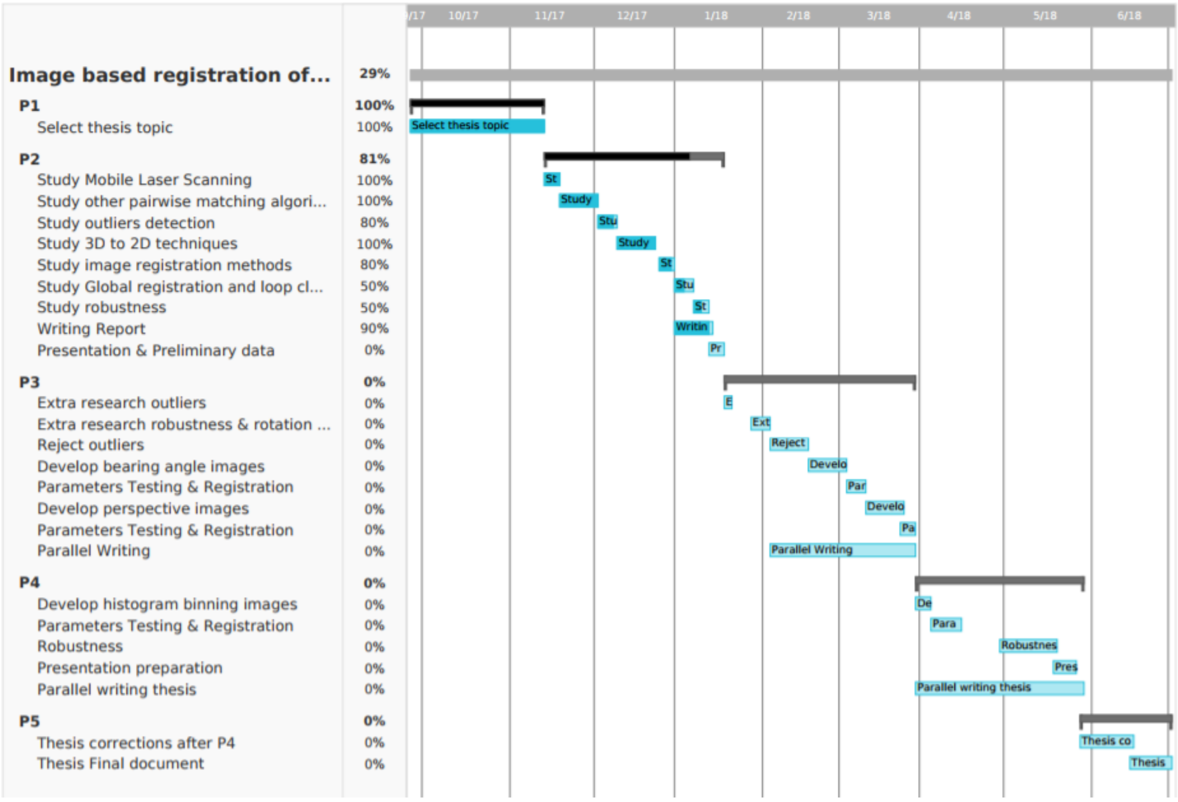

Figure 16: Time planning of the required activities.

6 Tools and datasets

6.1 Tools

Firstly, QTreader will be used to visualize the point clouds. LAStools which are command line tools will be used for decompressing the point clouds (from LAZ to LAS), for filtering and for clipping, if needed. The main tool for the images creation, registration, results comparison and analysis will be Python. Several libraries will be used, such as matplotlib, scipy for all the statistical needs of this project, and Numpy, OpenCV and PIL for the image generation, pixel manipulation, enhancement etc. Also PCL algorithms could be used for general point cloud manipulation. In addition, QGIS will be used for loading and processing all the spatial layers needed for assessing the robustness of the methods.

6.2 Datasets

The Mobile Laser Scanning data will be provided by the company CycloMedia. Namely, firstly the web viewer StreetSmart from the company is utilized in order to detect the id of the scan needed. Then by using the ids, the corresponding scans can be retrieved from the company's databases. For this project specifically, data from Schiedam in The Netherlands and Stuttgart in Germany will be used, since according to the experience of the supervisors, in those areas different and/or interesting cases can be found.

References

T. Bailey and H. Durrant-Whyte. Simultaneous localization and mapping (SLAM): part II. *IEEE Robotics Automation Magazine*, 13(3):108–117, September 2006. ISSN 1070-9932. doi: 10.1109/MRA.2006.1678144.

B. Barshan and H. F. Durrant-Whyte. Inertial navigation systems for mobile robots. *IEEE Transactions on Robotics and Automation*, 11(3):328–342, June 1995. ISSN 1042-296X. doi: 10.1109/70.388775.

Herbert Bay, Andreas Ess, Tinne Tuytelaars, and Luc Van Gool. Speeded-Up Robust Features (SURF). *Computer Vision and Image Understanding*, 110(3):346–359, June 2008. ISSN 1077-3142. doi: 10.1016/j.cviu.2007.09.014. URL `http://www.sciencedirect.com/science/article/pii/S1077314207001555`.

Ben Bellekens, Vincent Spruyt, Raf Berkvens, and Maarten Weyn. A Survey of Rigid 3d Point-cloud Registration Algorithms. August 2014.

J.-A Beraldin. Integration of Laser Scanning and Close-Range Photogrammetry - The Last Decade and Beyond. *Proceedings of the XXth ISPRS Congress*, January 2004.

P. J. Besl and N. D. McKay. A method for registration of 3-D shapes. *IEEE Transactions on Pattern Analysis and Machine Intelligence*, 14(2):239–256, February 1992. ISSN 0162-8828. doi: 10.1109/34.121791.

R. Blomley, M. Weinmann, J. Leitloff, and B. Jutzi. Shape distribution features for point cloud analysis - a geometric histogram approach on multiple scales. *ISPRS Annals of Photogrammetry, Remote Sensing and Spatial Information Sciences*, 3:9–16, August 2014. doi: 10.5194/isprsannals-II-3-9-2014. URL `http://adsabs.harvard.edu/abs/2014ISPAn.II3....9B`.

C. Brenner. Extraction of Features from Mobile Laser Scanning Data for Future Driver Assistance Systems. In *Proceedings of the 12th AGILE Conference*, Verlag Berlin Heidelberg, 2009. Springer. doi: 10.1007/978-3-642-00318-9_2.

Cartwright, W., Gartner, G., Meng, L., and Peterson, M.P. *Lecture Notes in Geoinformation and Cartography, Extraction of Features from Mobile Laser Scanning Data for Future Driver Assistance Systems*. Springer, 2009. URL `http://www.springer.com/series/7418`.

Y. Chen and G. Medioni. Object modelling by registration of multiple range images. *Image and Vision Computing*, 10(3):145–155, April 1992. ISSN 0262-8856. doi: 10.1016/0262-8856(92)90066-C. URL `http://www.sciencedirect.com/science/article/pii/026288569290066C`.

D. Chetverikov, D. Svirko, D. Stepanov, and P. Krsek. The Trimmed Iterative Closest Point algorithm. In *Object recognition supported by user interaction for service robots*, volume 3, pages 545–548 vol.3, 2002. doi: 10.1109/ICPR.2002.1047997.

L. Ding, A. Goshtasby, and M. Satter. Volume image registration by template matching. *Image and Vision Computing*, 19(12):821–832, October 2001. ISSN 0262-8856. doi: 10.1016/S0262-8856(00)00101-3. URL `http://www.sciencedirect.com/science/article/pii/S0262885600001013`.

Guy Godin, Marc Rioux, and Rejean Baribeau. Three-dimensional registration using range and intensity information. In *Proc. SPIE 2350, Videometrics III*, October 1994. doi: 10.1117/12.189139.

Norbert Haala, Michael Peter, Jens Kremer, and Graham Hunter. Mobile LIDAR Mapping for 3d Point Cloud Collection in Urban Areas - A Performance Test. *In: Proceedings of XXI ISPRS Congress, Beijing, China, July 3-11, 2008*, 37, July 2008.

F. R. Hampel. A General Qualitative Definition of Robustness. *The Annals of Mathematical Statistics*, 42(6):1887–1896, December 1971. ISSN 0003-4851, 2168-8990. doi: 10.1214/aoms/1177693054. URL `https://projecteuclid.org/euclid.aoms/1177693054`.

Yuqing He and Yuangang Mei. An efficient registration algorithm based on spin image for LiDAR 3d point cloud models. *Neurocomputing*, 151(Part 1):354–363, March 2015. ISSN 0925-2312. doi: 10.1016/j.neucom.2014.09.029. URL `http://www.sciencedirect.com/science/article/pii/S0925231214012120`.

A. E. Johnson and M. Hebert. Using spin images for efficient object recognition in cluttered 3d scenes. *IEEE Transactions on Pattern Analysis and Machine Intelligence*, 21(5):433–449, May 1999. ISSN 0162-8828. doi: 10.1109/34.765655.

Andrew Edie Johnson and Martial Hebert. Surface Matching for Object Recognition in Complex 3-D Scenes. *Image and Vision Computing*, 16:635–651, 1998.

Harri Kaartinen, Juha Hyyppä, Antero Kukko, Anttoni Jaakkola, and Hannu Hyyppä. Benchmarking the Performance of Mobile Laser Scanning Systems Using a Permanent Test Field. *Sensors*, 12(9):12814–12835, September 2012. doi: 10.3390/s120912814. URL `http://www.mdpi.com/1424-8220/12/9/12814`.

Alex Krause. Spin-Images: A Representation for 3-D Surface Matching, 1997. URL `https://www.ri.cmu.edu/publications/spin-images-a-representation-for-3-d-surface-matching/`.

A. Kukko, H. Kaartinen, J. Hyyppä, and Y. Chen. Multiplatform Mobile Laser Scanning: Usability and Performance. *Sensors*, 12(9):11712–11733, August 2012. doi: 10.3390/s120911712. URL `http://www.mdpi.com/1424-8220/12/9/11712`.

Marco Langerwisch and Bernardo Wagner. *Registration of Indoor 3D Range Images using Virtual 2D Scans.* January 2010.

Robert W. Levi and Thomas Judd. Dead reckoning navigational system using accelerometer to measure foot impacts, December 1996. URL `http://www.google.com/patents/US5583776`. U.S. Classification 701/400, 701/300, 701/494, 701/500; International Classification G01C22/00, G01P3/50, G01C21/12; Cooperative Classification G06K9/00348, G01P3/50, G01C22/006, G01C21/12, A43B3/0005, A61B5/1126; European Classification A43B3/00E, G01P3/50, G01C21/12, G01C22/00P, G06K9/00G1G.

Y. B. Liang, Y. Qiu, and T. J. Cui. Semiautomatic Registration of Terrestrial Laser Scanning Data Using Perspective Intensity Images. *IEEE Geoscience and Remote Sensing Letters*, 14(1): 28–32, January 2017. ISSN 1545-598X. doi: 10.1109/LGRS.2016.2624268.

Chien-Chou Lin, Yen-Chou Tai, Jhong-Jin Lee, and Yong-Sheng Chen. A novel point cloud registration using 2d image features. *EURASIP Journal on Advances in Signal Processing*, 2017(1):5, December 2017. ISSN 1687-6180. doi: 10.1186/s13634-016-0435-y. URL `https://link.springer.com/article/10.1186/s13634-016-0435-y`.

Martin Magnusson, Achim Lilienthal, and Tom Duckett. Scan registration for autonomous mining vehicles using 3d-NDT. *Journal of Field Robotics*, 24(10):803–827, October 2007. ISSN 1556-4967. doi: 10.1002/rob.20204. URL `http://onlinelibrary.wiley.com/doi/10.1002/rob.20204/abstract`.

A. A. Matkan, M. Hajeb, B. Mirbagheri, S. Sadeghian, and M. Ahmadi. Spatial Analysis for Outlier Removal from LIDAR Data. *ISPRS - International Archives of the Photogrammetry, Remote Sensing and Spatial Information Sciences*, 2:187–190, October 2014. doi: 10.5194/isprsarchives-XL-2-W3-187-2014. URL `http://adsabs.harvard.edu/abs/2014ISPAr.XL2..187M`.

R. Matungka, Y. F. Zheng, and R. L. Ewing. Image Registration Using Adaptive Polar Transform. *IEEE Transactions on Image Processing*, 18(10):2340–2354, October 2009. ISSN 1057-7149. doi: 10.1109/TIP.2009.2025010.

S. Mendenhall. Mobile laser scanning - Civil + Structural Engineer magazine. *CE News*, January 2014. URL `https://csengineermag.com/article/mobile-laser-scanning/`.

C. Padia and N. Pears. A Review and Characterization of ICP-based Symmetry Plane Localisation in 3d Face Data. December 2017.

Gang Pang. *Outlier detection and data filtering in LiDAR data with multiple attributes*. Thesis, The Hong Kong Polytechnic University, 2011. URL `http://ira.lib.polyu.edu.hk/handle/10397/4961`.

François Pomerleau, Francis Colas, Roland Siegwart, and Stéphane Magnenat. Comparing ICP variants on real-world data sets. *Autonomous Robots*, 34(3):133–148, April 2013. ISSN 0929-5593, 1573-7527. doi: 10.1007/s10514-013-9327-2. URL `https://link.springer.com/article/10.1007/s10514-013-9327-2`.

I. Puente, H. González-Jorge, P. Arias, and J. Armesto. Land-Based Mobile Laser Scanning Systems: a Review. *ISPRS - International Archives of the Photogrammetry, Remote Sensing and Spatial Information Sciences*, 3812:163–168, September 2011. doi: 10.5194/isprsarchives-XXXVIII-5-W12-163-2011. URL `http://adsabs.harvard.edu/abs/2011ISPAr3812W.163P`.

P. J. Rousseeuw. Least Median of Squares Regression. *Journal of the American Statistical Association*, 79(388):871–880, December 1984. ISSN 0162-1459. doi: 10.1080/01621459.1984.10477105. URL `http://www.tandfonline.com/doi/abs/10.1080/01621459.1984.10477105`.

Peter Rousseeuw. Multivariate Estimation With High Breakdown Point. *Mathematical Statistics and Applications Vol. B*, pages 283–297, January 1985. doi: 10.1007/978-94-009-5438-0_20.

Peter J. Rousseeuw and Mia Hubert. Robust statistics for outlier detection. *Wiley Interdisciplinary Reviews: Data Mining and Knowledge Discovery*, 1(1):73–79, January 2011. ISSN 1942-4795. doi: 10.1002/widm.2. URL `http://onlinelibrary.wiley.com/doi/10.1002/widm.2/abstract`.

Peter J. Rousseeuw and Annick M. Leroy. *Robust Regression and Outlier Detection*. John Wiley & Sons, February 2005. ISBN 978-0-471-72537-4.

D. Scaramuzza, A. Harati, and R. Siegwart. Extrinsic self calibration of a camera and a 3d laser range finder from natural scenes. In *2007 IEEE/RSJ International Conference on Intelligent Robots and Systems*, pages 4164–4169, October 2007. doi: 10.1109/IROS.2007.4399276.

Aleksandr V. Segal, Dirk Haehnel, and Sebastian Thrun. Generalized-ICP. In *Proceedings of Robotics: Science and Systems.*, Seattle, 2009.

G. C. Sharp, S. W. Lee, and D. K. Wehe. ICP registration using invariant features. *IEEE Transactions on Pattern Analysis and Machine Intelligence*, 24(1):90–102, January 2002. ISSN 0162-8828. doi: 10.1109/34.982886.

A. Shetty. *GPS-LiDAR sensor fusion aided by 3D city models for UAVs*. PhD thesis, University of Illinois at Urbana-Champaign, April 2017. URL `http://hdl.handle.net/2142/97501`.

S. Sotoodeh. Outlier detection in laser scanner point clouds. In *International Archives of Photogrammetry, Remote Sensing and Spatial Information Sciences XXXVI-5*, pages 297–302, 2006.

Paridhi Swaroop and Neelam Sharma. *An Overview of Various Template Matching Methodologies in Image Processing*, volume 153. November 2016. DOI: 10.5120/ijca2016912165.

E. Trucco, A. Fusiello, and V. Roberto. Robust motion and correspondence of noisy 3-D point sets with missing data. *Pattern Recognition Letters*, 20(9):889–898, September 1999. ISSN 0167-8655. doi: 10.1016/S0167-8655(99)00055-0. URL `http://www.sciencedirect.com/science/article/pii/S0167865599000550`.

Farhan Ullah and Shun'ichi Kaneko. Using orientation codes for rotation-invariant template matching. *Pattern Recognition*, 37(2):201–209, February 2004. ISSN 0031-3203. doi: 10.1016/S0031-3203(03)00184-5. URL `http://www.sciencedirect.com/science/article/pii/S0031320303001845`.

J. Á. Víšek. Advantages and disadvantages, challenges and threads of robust methods. In *Proceedings of the seminar "Analyza dat 2012/II" (Data Analysis 2012/II), 14. - 16. 11. 2012, Trilobyte Statistica Software (http://www.trilobyte.cz), 121 - 150.*, Pardubice, 2012. ISBN 978-80-904053-6-3.

Wang C., Cho Y. K., and Park J. W. Performance Tests for Automatic 3d Geometric Data Registration Technique for Progressive As-Built Construction Site Modeling. *Computing in Civil and Building Engineering (2014)*, 2014. ISSN 9780784413616. doi: 10.1061/9780784413616.131. URL `https://ascelibrary.org/doi/abs/10.1061/9780784413616.131`.

B. Wei, F. Wang, and X. Hu. Rotation-invariant template matching based on ring projection and orientation codes. In *Fifth International Conference on Intelligent Control and Information Processing*, pages 192–197, August 2014. doi: 10.1109/ICICIP.2014.7010338.

P. Čížek and J.A. Visek. *Least Trimmed Squares*. Humboldt-Univ., 2000. Google-Books-ID: UDBzYgEACAAJ.